

# 1 Sedimentation and soil carbon accumulation in 2 degraded mangrove forests of North Sumatra, Indonesia

3 Daniel Murdiyarso<sup>1,2\*</sup>, Bayu Budi Hanggara<sup>1</sup>, and Ali Arman Lubis<sup>3</sup>

4 <sup>1</sup> Center for International Forestry Research, Jl. CIFOR, Situ Gede, Bogor 16115, Indonesia

5 <sup>2</sup> Department of Geophysics and Meteorology, Bogor Agricultural University, Bogor, 16680, Indonesia

6 <sup>3</sup> Center for Application of Isotope and Radiation, National Nuclear Energy Agency of Indonesia, Jakarta  
7 12710, Indonesia

8  
9 \* [d.murdiyarso@cgiar.org](mailto:d.murdiyarso@cgiar.org)

## 10 11 Abstract

12 Mangrove ecosystems are often referred to as “land builders” because of their ability to trap  
13 sediments transported from the uplands as well as from the oceans. The sedimentation process in  
14 mangrove areas is influenced by hydro-geomorphic settings that represent the tidal range and coastal  
15 geological formation. We estimated the sedimentation rate in North Sumatran mangrove forests using  
16 the <sup>210</sup>Pb radionuclide technique, also known as the constant rate supply method, and found that  
17 mudflats, fringes, and interior mangroves accreted  $4.3 \pm 0.2$  mm yr<sup>-1</sup>,  $5.6 \pm 0.3$  mm yr<sup>-1</sup>, and  $3.7 \pm 0.2$  mm  
18 yr<sup>-1</sup>, respectively. Depending on the subsurface changes, these rates could potentially keep pace with  
19 global sea level rise of 2.6–3.2 mm yr<sup>-1</sup>, except the interior mangrove they would also be able to cope  
20 with regional sea-level rise of  $4.2 \pm 0.4$  mm yr<sup>-1</sup>. The mean soil carbon accumulation rates in the  
21 mudflats, fringes, and interior areas were  $40.1 \pm 6.9$  g C m<sup>-2</sup>yr<sup>-1</sup>,  $50.1 \pm 8.8$  g C m<sup>-2</sup>yr<sup>-1</sup>, and  $47.7 \pm 12.5$  g C

22  $\text{m}^{-2}\text{yr}^{-1}$ , respectively, much lower than the published global average of  $226 \pm 39 \text{ g C m}^{-2}\text{yr}^{-1}$ . We also  
23 found that based on the excess of radioactive elements derived from atomic bomb fallout, the sediment  
24 in the mudflat area was deposited since over 28 years ago, and is much younger than the sediment  
25 deposited in the interior and fringe areas that are 43 years 54 years old, respectively.

26 Keywords: hydro-geomorphology, radionuclide, sea-level rise, land building, sediment age

27

## 28 Introduction

29 Mangrove ecosystems provide numerous invaluable services including supporting (nutrient  
30 cycling, net primary production, and land formation), provisioning (food, fuel, and fiber), and regulating  
31 (climate, flood, storm surges, and pollution) services [1-5]. Situated in a transition zone between  
32 terrestrial and oceanic environments, mangrove forests play particularly important roles in moderating  
33 fresh water flow from the upland, while buffering against tidal ranges of the sea and saline water [6].  
34 The unique shape and form of the root systems of mangrove species enable them to trap and  
35 accumulate sediments, which often contain large quantities of organic carbon [7-9]. This ability is  
36 influenced by local hydrology, geography, and topography [9,10]. In some cases, sedimentation is  
37 followed by colonization, expansion, and migration of pioneering mangrove species [11]. Therefore,  
38 carbon sequestration and storage above and below ground in mangrove ecosystems are effective in  
39 mitigating climate change [2,4].

40 The sustainability of the services that mangroves, including those in North Sumatra, provide is  
41 facing increasing pressure from aquaculture and agricultural development [12]. In addition, climate  
42 change and its impacts on sea-level rise have increased coastal vulnerability to erosion and inundation.  
43 Sea level has risen more than 5 cm over the last 20 years or  $3.2 \text{ mm yr}^{-1}$  on average—a rate that has

44 nearly doubled since 1990 [13,14]—and is expected to continue to increase in the future [15]. Although  
45 mangrove tree species are able to tolerate inundation by tides, they can die and their habitat formation  
46 can be damaged if, as a result of sea-level rise, the frequency and duration of the inundation exceeds  
47 their specific physiological thresholds [16,17]. Sedimentation in coastal areas that is facilitated by  
48 mangrove forests demonstrates that mangroves are “land builders” [7] and can adapt to rising sea  
49 levels. The rate of sedimentation can be an important factor to determine the sustainability of  
50 mangrove management.

51 The  $^{210}\text{Pb}$  radionuclide dating technique is employed to estimate sedimentation using a  
52 geochronology approach.  $^{210}\text{Pb}$  dating methods are an invaluable tool for recent (~100 years)  
53 geochemical studies [18,19]. The natural  $^{210}\text{Pb}$  radionuclide is measured from each sediment interval as  
54 the ratio between  $^{209}\text{Po}$  and  $^{210}\text{Pb}$ , both radionuclides originate from the decay of uranium ( $^{238}\text{U}$ ) [20,  
55 21]. In the process of decaying  $^{210}\text{Pb}$ , it is known that there are supported  $^{210}\text{Pb}$  and unsupported  $^{210}\text{Pb}$ .  
56 Supported  $^{210}\text{Pb}$  is formed by the decay of  $^{226}\text{Ra}$  in eroded parent rock and accumulates in the  
57 sediments. The level of supported  $^{210}\text{Pb}$  in an ecosystem is generally differ very little because it comes  
58 from the same parent rock. Unsupported  $^{210}\text{Pb}$  accumulates in sediments that enter the ecosystem [21].  
59 This technique has frequently been used to investigate study short-term sedimentation and carbon  
60 accumulation rates [14,18,22,23]; however, it is not appropriate for long-term sediment accumulation (>  
61 100 years) [24].

62 Rapid development in coastal areas due to anthropogenic activity is threatening vertical accretion  
63 and horizontal expansion of sediment in mangrove forests. These impacts include altered hydrological  
64 patterns, sedimentation, and nutrient loads that result from disturbances that restrict hydrological  
65 connections [14,25,26]. It is therefore important to understand the process of sedimentation, especially  
66 in degraded and threatened mangroves.

67 This study was designed to quantify the rates of sedimentation and carbon accumulation in  
68 degraded mangrove forests in Deli Serdang regency, a low-lying coastal zone in North Sumatra,  
69 Indonesia. The region is influenced by the effluent of the large city of Medan and the busy harbor port  
70 of Belawan (see [Fig 1](#)). Surrounded by shrimp ponds and newly developed oil palm plantations, the  
71 remaining mangroves in Sei Percut experience tremendous environmental pressure.

72

73 **Fig 1. Study area of mangrove forests in Deli Serdang regency, North Sumatra, Indonesia.**

74

75 The mangroves are dominated by *Avicennia* sp. and *Rhizophora* sp. Besides natural colonization of  
76 *Avicennia* sp. in the mudflat area, restoration has also been attempted, in the mudflats and in the  
77 abandoned and active ponds in the interior.

78

## 79 Methods

### 80 Site selection

81 The site selected is located at 3°46'15.56–3°42'53.32 N and 98°42'28.23–98°47'22.33b E. It is  
82 characterized by a monsoonal tropical climate with a mean temperature of 30°C and annual rainfall of  
83 1848 mm [27]. The sea tide ranges from 0.9 to 2.6 m with a diurnal pattern influenced by the Andaman  
84 Sea. We selected three hydro-geomorphic settings representing mudflat, fringing mangrove and interior  
85 mangrove areas as shown in [Fig 1](#). Three core soil samples were collected from these settings to capture  
86 the sedimentation processes and carbon storage.

## 87 Sediment sampling and sample preparation

88 The sampling point in the mudflat was located approximately 15 m from the coastline (or fringe  
89 zone) and the interior at around 375 m from the coastline. Soil cores at each hydro-geomorphic setting  
90 were collected to a depth of 50 cm and sliced at 2 cm intervals for the first 10 cm and then 5 cm  
91 intervals (see [Fig 2](#)).

92

### 93 **Fig 2. Soil core for sediment sampling in the first 50 cm below the surface.**

94

95 The samples were oven-dried at a temperature of 40°C (to avoid oxidation of carbon) until a  
96 constant weight was reached. Each sample was homogenized using a mortar and pestle. Samples were  
97 dried, crushed and sieved through 120 ( $\phi = 0.125$  mm) mesh size (cohesive sediment). Roots and other  
98 material containing calcareous sediments were removed. Bulk density was determined for each interval  
99 by dividing the dry weight by the sample volume. The analysis of carbon content of the sediments was  
100 carried out employing a combustion method using *TruSpec Analysis CHNS* for each layer.

## 101 Sediment accumulation rate

102 The sediment accumulation rates were calculated using a constant rate of supply (CRS) method  
103 [21]. Approximately 5 g dried sediment combined with 0.2 ml of radioactive tracer of  $^{209}\text{Po}$  were  
104 dissolved in a 10 ml of HCl (1:1), 10 ml of  $\text{HNO}_3$ , 15 ml of  $\text{H}_2\text{O}$  and 5–6 drops of 30%  $\text{H}_2\text{O}_2$  and dried over  
105 a water bath at 80°C. A volume of 10 ml of HCl (1:1) and 40 ml of distilled water was added to the dry  
106 residue, before reheating over the water bath for approximately 10 minutes. The solution was filtered  
107 through filter paper No. 42 to remove sediment and rinsed with 30 ml of 0.3N HCl. The filtrate was then  
108 dried over the water bath. Volumes of 4 ml of HCl (1:1) and 50 ml of 0.3N HCl were added to the dry

109 residue. Then 400 mg of ascorbic acid was added to complex out any dissolved iron present that might  
110 interfere with the plating processing of the Po isotopes. The sediment solution was then plated onto a  
111 2.2 cm diameter copper disk. Po isotopes were quantified using a Canberra Alpha Spectrometer, Model  
112 7401 with Passivated Implanted Planar Silicon detector Type A450 20AM. Measurements were carried  
113 out until a Gaussian spectrum was obtained (standard deviation was less than 10%).

114 To account for variability in sedimentation throughout time, the CRS model, developed by  
115 Appleby [21], was employed to calculate sediment age.

$$116 \quad A(x) = A(o)e^{-kt} \quad (1)$$

117 where  $A(x)$  is the unsupported  $^{210}\text{Pb}$  activity below the individual segment being dated ( $\text{Bq kg}^{-1}$ ),  $A(o)$  is  
118 the total unsupported  $^{210}\text{Pb}$  activity in the soil column ( $\text{Bq kg}^{-1}$ ),  $k$  is the  $^{210}\text{Pb}$  decay constant ( $0.0311 \text{ yr}^{-1}$ ), and  $t$  is the age of sediments (yr) at each segment. This can be obtained from:

$$120 \quad t = \frac{1}{k} \ln \frac{A(o)}{A(x)} \quad (2)$$

121 The constant supply of unsupported  $^{210}\text{Pb}$  ( $\text{Bq m}^{-2}$ ),  $C$ , was used to estimate sediment  
122 accumulation rate,  $r$  ( $\text{kg m}^{-2}\text{yr}^{-1}$ ) at a certain segment and calculated as:

$$123 \quad r = \frac{kA}{C} \quad (3)$$

124 To obtain the sediment accretion rate ( $\text{mm yr}^{-1}$ ), the sediment accumulation ( $\text{g m}^{-2} \text{ yr}^{-1}$ ) was divided by  
125 soil the bulk density,  $BD$  ( $\text{g cm}^{-3}$ ).

126 Following Marchio et al. [22], the soil carbon accumulation rate,  $C_{\text{acc}}$  ( $\text{g C m}^{-2} \text{ yr}^{-1}$ ) was calculated  
127 for each hydro-geomorphic setting as:

$$128 \quad C_{\text{acc}} = A_d \times BD \times C_{\text{conc}} \quad (4)$$

129           Where  $A_d$  is the sediment accretion rate at a certain layer ( $\text{cm yr}^{-1}$ ), and  $C_{conc}$  ( $\text{g C g-soil}^{-1}$ ) is the  
130 average soil carbon concentrations of the same layer.

## 131 Results

### 132 Bulk density and soil carbon content

133           Bulk density ( $BD$ ) and soil carbon content are shown in Fig 3. Their variation with depth in all  
134 hydro-geomorphic locations showed opposing trends, with  $BD$  increasing with depth, while carbon  
135 content decreased.  $BD$  ranged between  $0.36 \text{ g cm}^{-3}$  and  $0.77 \text{ g cm}^{-3}$  with the widest range found in the  
136 interior ( $0.36\text{--}0.74 \text{ g cm}^{-3}$ ), followed by the mudflat ( $0.43\text{--}0.77 \text{ g cm}^{-3}$ ). The narrowest range was found  
137 in the fringing mangrove ( $0.40\text{--}0.55 \text{ g cm}^{-3}$ ). In general, the variation of  $BD$  is within the range of most  
138 mangrove forests found across Indonesia [4].

139           On average, mudflat and interior mangroves had similar  $BD$ s of  $0.60 \pm 0.11 \text{ g cm}^{-3}$  and  $0.60 \pm 0.12$   
140  $\text{g cm}^{-3}$ , respectively, with much lower  $BD$  in the fringing mangrove of  $0.46 \pm 0.05 \text{ g cm}^{-3}$ . These values  
141 suggest that the hydro-geomorphic setting dictates how sediments settle, are compacted and disturbed  
142 (or protected) by the hydrodynamics of the sea and fluvial water.

143

144 **Fig 3. Bulk density ( $\text{g cm}^{-3}$ ) and soil carbon content (%C) at different hydro-geomorphic settings in**  
145 **mangrove forests in Deli Serdang, North Sumatra.**

146

147           The average soil carbon content of Deli Serdang mangroves across the hydro-geomorphic setting  
148 ranged between 1.5% (mudflat) and 3.0% (interior), with fringe mangroves having an intermediate  
149 carbon content of 2.0%. This distribution signifies the role of mangrove vegetation as the primary source  
150 of carbon. Deposited and decomposed litter and decayed fine roots contribute to the *in-situ* organic

151 carbon. These figures are far lower than the figures found in undisturbed mangroves in Sumatra (9.4%),  
152 Kalimantan (9.7%), and Sulawesi (15.6%). Moreover, they are even lower than degraded mangroves on  
153 Java of 5.6% [4].

#### 154 $^{210}\text{Pb}$ radionuclide activity and sediment age

155 The unsupported  $^{210}\text{Pb}$  activity in Deli Serdang mangroves is shown in Fig 4. The mudflat area  
156 values ranged between  $44.0 \pm 1.8 \text{ Bq kg}^{-1}$  and  $66.9 \pm 3.7 \text{ Bq kg}^{-1}$ . In the fringe mangroves, they ranged  
157 between  $35.1 \pm 1.8 \text{ Bq kg}^{-1}$  and  $75.7 \pm 4.2 \text{ Bq kg}^{-1}$ , while the interior mangroves ranged from  $39.9 \pm 2.2$   
158  $\text{Bq kg}^{-1}$  to  $78.7 \pm 4.3 \text{ Bq kg}^{-1}$ .

159

160 **Fig 4.  $^{210}\text{Pb}$  activity in the sediment across hydro-geomorphic setting of mangrove forests in Deli**  
161 **Serdang, North Sumatra: (a) mudflat, (b) fringe, (c) interior.** The grey bars represent total  
162 activity of  $^{210}\text{Pb}$  (supported + unsupported), whereas the black bars represent supported  $^{210}\text{Pb}$   
163 activity derived from the lowest activity found in the sample. The supported  $^{210}\text{Pb}$  was formed  
164 from decayed  $^{226}\text{Ra}$  in eroded parent rock and accumulated in the sediments, and the  
165 unsupported  $^{210}\text{Pb}$  was formed from decayed  $^{222}\text{Rn}$  in nature and accumulated in the sediment.

166

167 The total  $^{210}\text{Pb}$  activity in the mudflat and fringe in the upper layer fluctuated because there was  
168 no vegetation binding the sediment on the mudflat area, so they are subject to the influence of currents  
169 and waves producing fluctuations in the suspended sediment in the area. In the fringe area, the  
170 variation was due to the influence of watersheds and less well-established root systems of colonizing  
171 mangrove seedlings.



172 The supported  $^{210}\text{Pb}$  activity values were obtained from the lowest unsupported values [28]. Their  
173 variation across hydro-geomorphic settings was relatively small. The values in the mudflat, fringe, and  
174 interior were  $44.0 \pm 3.7 \text{ Bq kg}^{-1}$ ,  $35.1 \pm 2.3 \text{ Bq kg}^{-1}$ , and  $42.1 \pm 1.9 \text{ Bq kg}^{-1}$ , respectively. However, due to  
175 the limitations of CRS analysis the depth of the core that could be analysed was up to 8 cm, 25 cm and  
176 10 cm for the mudflat, fringe and interior settings. Nevertheless, the CSR is the least arguable method  
177 compared with mass balance method, as it measures the vertical decline of  $^{210}\text{Pb}$  concentration and  
178 provides a chronology of sedimentation for up to the past century [29].

179 The estimates of sediment age in each layer and at all hydro-geomorphic settings are shown in Fig  
180 5. The oldest sediment was found in the fringing mangroves, which was formed  $54.7 \pm 3.2$  yrs ago  
181 (around 1961) at 25 cm deep, followed by the interior mangroves of  $43.1 \pm 2.3$  yrs (around 1973) at a  
182 depth of 10 cm. The youngest sediment was formed  $28.4 \pm 1.6$  yrs ago (around 1988) found in the  
183 mudflat area at 8 cm deep. These ages of sedimentation in North Sumatra are much younger than those  
184 found in Everglades National Park in the Gulf of Mexico, where the sedimentation processes began in  
185 1926 [23]. Since the region was very much affected by high storm surges, the sediment deposits and  
186 carbon burial were relatively higher.

187

188 **Fig 5. Sediment accumulation rate and the age of sediment in each hydro-geomorphic setting of**  
189 **mangrove forests in Deli Serdang, North Sumatra: (a) mudflat, (b) fringe, (c) interior.** The  
190 oldest sediment was found in the fringe mangroves of about 55 years.

191

192 Sediment accretion and soil carbon accumulation rates

193 The constant supply of unsupported  $^{210}\text{Pb}$  is used to estimate sediment accumulation rate (mass  
194 per unit area) or sediment accretion rate (thickness). This is a good indicator of growth capacity,

195 horizontal expansion of mangrove ecosystems, and, to some extent, effectiveness as carbon sinks and  
196 disturbance regimes [23]. Fig 6a shows sediment accretion and soil carbon accumulation rates in all  
197 hydro-geomorphic settings with fringing mangroves being the largest ( $5.6 \pm 0.3 \text{ mm yr}^{-1}$ ), followed by  
198 mudflats at  $4.3 \pm 0.2 \text{ mm yr}^{-1}$ , and interior mangroves at  $3.7 \pm 0.2 \text{ mm yr}^{-1}$ . This pattern is associated  
199 with the size, shape, and spatial distribution of trees. The rate increases with increasing density of trees  
200 especially those of *Rhizophora sp.* and their complex root systems, which not only trap the mud but  
201 most likely also allows them to withstand greater sedimentation. This was particularly the case for  
202 fringing mangroves as the interior mangroves were isolated from receiving sediments. The  
203 sedimentation in the mangroves of Deli Serdang, North Sumatra was generally due to marine and river  
204 sedimentary deposits. These results are in line with previous work, which generally found that  
205 sedimentation rate was the highest along the coastline and decreased in the area near the mainland  
206 [11].

207

208 **Fig 6. Sediment accretion rate (a) and soil carbon accumulation rate (b) in each hydro-geomorphic**  
209 **setting of mangrove forests in Deli Serdang, North Sumatra: mudflat, fringe, and interior.** It is  
210 shown in (a) that sedimentation rate in all settings can cope with global sea level rise (SLR) but  
211 only interior mangroves cannot cope with regional SLR.

212

213 The accumulation rate of soil carbon depends on sedimentation rate,  $BD$ , and the carbon  
214 concentration of sediment. As shown in Fig 6b the average value of soil carbon accumulation in the  
215 mudflat area was  $40.1 \pm 6.9 \text{ g C m}^{-2}\text{yr}^{-1}$ . In the fringe mangroves, it was  $50.1 \pm 88.4 \text{ g C m}^{-2}\text{yr}^{-1}$ , and in the  
216 interior mangroves was  $47.7 \pm 12.5 \text{ g C m}^{-2}\text{yr}^{-1}$ . Although mudflat zone demonstrates higher  
217 sedimentation rate than interior mangroves, the accumulation of carbon is lower. This is because the  
218 presence of mangrove forest is an important source of autochthonous carbon. However, the rate of

219 carbon burial across the hydro-geomorphic shown in Deli Serdang mangroves are very low compared  
220 with the global average of around  $226 \pm 39 \text{ g C m}^{-2}\text{yr}^{-1}$  [30].

## 221 Discussion

222 Reduction of land-based emissions, such as reducing emissions from deforestation and forest  
223 degradation, known as REDD+ is often promoted as climate mitigation measures. Mangrove forest is a  
224 unique example by which climate change mitigation can be simultaneously implemented with adaption  
225 strategies. Combining the two roles could even be more attractive for stakeholders at national level to  
226 demonstrate the nationally determined contributions (NDCs) as stipulated in the Paris Agreement,  
227 where climate change adaptation and mitigation are implemented in a balanced manner. Moreover, sub  
228 national and local agenda could even be built around adaptation strategies that usually gain less  
229 attention in both programming and budgeting processes.

230 Mangroves promote adaption to rising sea level

231 The global average sedimentation rate in mangrove forests ranges between  $0.1$  and  $10.0 \text{ mm yr}^{-1}$ ,  
232 with a median value of  $5 \text{ mm yr}^{-1}$  [31, 32]. Based on  $^{210}\text{Pb}$  radionuclide analysis using the CRS method we  
233 found an average rate of sediment accretion rate in the mudflat area of  $4.3 \pm 0.2 \text{ mm yr}^{-1}$ , while in the  
234 fringe mangroves the rate was  $5.6 \pm 0.3 \text{ mm yr}^{-1}$ , and the lowest rate was found in the interior  
235 mangroves of  $3.7 \pm 0.2 \text{ mm yr}^{-1}$ . Assuming that no sub surface changes took place, sedimentation in Deli  
236 Serdang mangrove forests can keep pace with global sea-level rise of  $2.6\text{--}3.2 \text{ mm yr}^{-1}$  [33] and regional  
237 sea-level rise of  $4.2 \pm 0.4 \text{ mm yr}^{-1}$  [15], except for the interior mangroves, which would not withstand  
238 the regional sea-level rise.

239 However, various processes can cause changes in mangrove sediment, including surface and  
240 subsurface processes. Previous studies [34, 35] describe processes occurring on or above the surface of

241 mangrove soils, including sedimentation (deposition of material to the soil surface), accretion (binding  
242 of this material in place), and erosion (loss of surface material). We did not monitor the sub surface  
243 processes, such as growth and decomposition of roots, soil swelling and shrinking associated with  
244 moisture content, and compaction, compression, and rebound of soils due to changes in the weight of  
245 the overlying material. In addition, at a larger scale, subsidence or geological movement may affect the  
246 sediment [36]. These mean that sediment accretion alone is not the best predictor of mangrove forests'  
247 resilience or capacity to adapt to sea-level rise. Measurement using the rod surface elevation table  
248 combined with a marker horizon may give further information [37].

249 Up to 80% of the sediments delivered by the tides are retained in mangrove forests [32, 38],  
250 enhancing mangrove colonization and expansion. The morphology and root systems of mangrove  
251 vegetation with their strong and complex shapes facilitates the trapping of sediment particles along the  
252 tidal ranges in the coastal area [38]. Natural regeneration, therefore, should be promoted.

## 253 Effectiveness of mangroves in mitigating climate change

254 Globally, organic carbon burial in coastal wetlands, including mangrove ecosystems, varies hugely  
255 depending on carbon content of the sediment deposited, net primary production, root and microbial  
256 activities, tidal waves and hydrodynamics, and hydro-geomorphic settings. It is generally accepted that  
257 the burial rate of soil sediments in mangrove ecosystems accumulates carbon between 163 and 265 g C  
258  $\text{m}^{-2}\text{yr}^{-1}$  [22,31,39-42]. These are the largest among any terrestrial ecosystems after saltmarsh [39].

259 Although carbon accumulation from sediment in mangrove forests in Deli Serdang, North Sumatra  
260 was very low (40-50 g C  $\text{m}^{-2}\text{yr}^{-1}$ ), seem to have significantly low carbon burial rates, it was reported that  
261 mangroves in Hinchinbrook Channel, Australia has an even lower average rate of 26 g C  $\text{m}^{-2}\text{yr}^{-1}$  [43]. In  
262 contrast, an extremely high rate of 949 g C  $\text{m}^{-2}\text{yr}^{-1}$  was found in Tamandare, Brazil [44].

263           The colonization, recruitment, and expansion of mangrove species vegetation in newly reclaimed  
264 land could gradually increase carbon sequestration through photosynthesis by the mangroves and litter  
265 deposition. Rehabilitation or restoration of mangrove to recover the carbon storage capacity of the  
266 ecosystem will take long time; therefore conserving intact mangroves is crucial and more effective to  
267 mitigate climate change.

268           These observations suggest that in terms of management, there is no one single solution for  
269 restoring degraded mangroves. A combination of methods and objectives could be explored to answer  
270 particular site-specific challenges. To some extent ecosystem services capable of accommodating a  
271 number of objectives and interests of multiple stakeholders. Ecosystem services provided by mangroves  
272 are among the candidates that attract local governments and community, including fishing community  
273 (nursery ground, coastal protection and pollution filtering), urban community (regulating micro-climate,  
274 cultural and education objects).

275

## 276 **Acknowledgements**

277 This study was part of the Sustainable Wetlands Adaptation and Mitigation Program (SWAMP) funded  
278 by the United States Agency for International Development (*AID-BFS-IO-17-00005*). The field work  
279 facilitated by the Yagasu Foundation and their field staff is gratefully acknowledged. The immense  
280 support of the staff at the Center of Isotopes and Radiation Application, National Nuclear Agency is  
281 recognized and thanked. Finally, we thank two anonymous reviewers for the very helpful comments  
282 that greatly improved this manuscript.

283

284

## 285 Author Contributions

286

287 **Conceptualization:** Daniel Murdiyarso.

288 **Data curation:** Daniel Murdiyarso.

289 **Formal analysis:** Daniel Murdiyarso and Bayu Budi Hanggara.

290 **Funding acquisition:** Daniel Murdiyarso.

291 **Investigation:** Daniel Murdiyarso and Bayu Budi Hanggara.

292 **Methodology:** Daniel Murdiyarso, Bayu Budi Hanggara, and Ali Arman Lubis.

293 **Project administration:** Daniel Murdiyarso.

294 **Supervision:** Daniel Murdiyarso and Ali Arman Lubis.

295 **Validation:** Daniel Murdiyarso and Ali Arman Lubis.

296 **Visualization:** Daniel Murdiyarso and Bayu Budi Hanggara.

297 **Writing ± original draft:** Daniel Murdiyarso, Bayu Budi Hanggara, and Ali Arman Lubis.

298 **Writing ± review & editing:** Daniel Murdiyarso

299

## 300 References

301 1. Millennium Ecosystem Assessment. *Ecosystems and Human Well-being: Wetlands and Water*

302 *Synthesis*. World Resources Institute: Washington, DC. 2005.

303 2. Donato DC, Kauffman JB, Murdiyarso D, Kurnianto S, Stidham M and Kanninen M. Mangrove among

304 the most carbon-rich forests in the tropics. *Nature Geosci.* 2011; 4: 293-297.

- 305 3. Webb EL, Friess DA, Krauss KW, Cahoon DR, Guntenspergen GR, and Phelps J. A global standard for  
306 monitoring coastal wetland vulnerability to accelerated sea level rise. *Nature Climate Change*. 2013.  
307 doi: [10.1038/NCLIMATE1756](https://doi.org/10.1038/NCLIMATE1756)
- 308 4. Murdiyarso D, Purbopuspito J, Kauffman JB, Warren MW, Sasmito SD, Donato DC, Manuri S,  
309 Krisnawati H, Taberima S, and Kurnianto S. The potential of Indonesian mangrove forest for global  
310 climate change mitigation. *Nature Climate Change*. 2015. doi: [10.1038/NCLIMATE2734](https://doi.org/10.1038/NCLIMATE2734)
- 311 5. Van Loon AF, Te Brake B, Van Huijgeveert MHJ, and Dijkema R. Hydrological classification, a practical  
312 tool for mangrove restoration. *PloS ONE*. 2016; 11: 3.  
313 doi: [10.1371/journal.pone.0150302](https://doi.org/10.1371/journal.pone.0150302)
- 314 6. Adame MF and Lovelock CE. Carbon and nutrient exchange of mangrove forest with the coastal  
315 ocean. *Hydrobiologia*. 2011; 663: 23-50. doi:[10.1007/s10750-010-0554-7](https://doi.org/10.1007/s10750-010-0554-7)
- 316 7. Alongi DM. Mangrove forests: Resilience, protection from tsunamis, and responses to global climate  
317 change. *Estuarine Coastal and Shelf Science*. 2008. doi: [10.1016/j.ecss.2007.08.024](https://doi.org/10.1016/j.ecss.2007.08.024)
- 318 8. Perry CT, Berkeley A, and Smithers SG. Microfacies characteristics of a tropical. Mangrove-fringed  
319 shoreline, Cleveland bay, Queensland, Australia: sedimentary and taphonomic controls on mangrove  
320 facies development. *Journal of Sedimentary Resear*. 2008. doi: [10.2110/jsr.2008.015](https://doi.org/10.2110/jsr.2008.015)
- 321 9. Sanders CJ, Smoak JM, Naidu A Sathy, Sanders LM, and Patchineelam SR. Organic carbon burial in a  
322 mangrove forest, margin and intertidal mud flat. *Estuarine, Coastal and Shelf Science*. 2010; 90  
323 (3):168–172. doi: [10.1016/j.ecss.2010.08.013](https://doi.org/10.1016/j.ecss.2010.08.013)
- 324 10. Ezcurra P, Ezcurra E, Garcillán PP, Costa MT, and Aburto-Oropeza O. Coastal landforms and  
325 accumulation of mangrove peat increase carbon sequestration and storage. *PNAS*. 2016.  
326 doi:[10.1073/pnas.1519774113](https://doi.org/10.1073/pnas.1519774113).

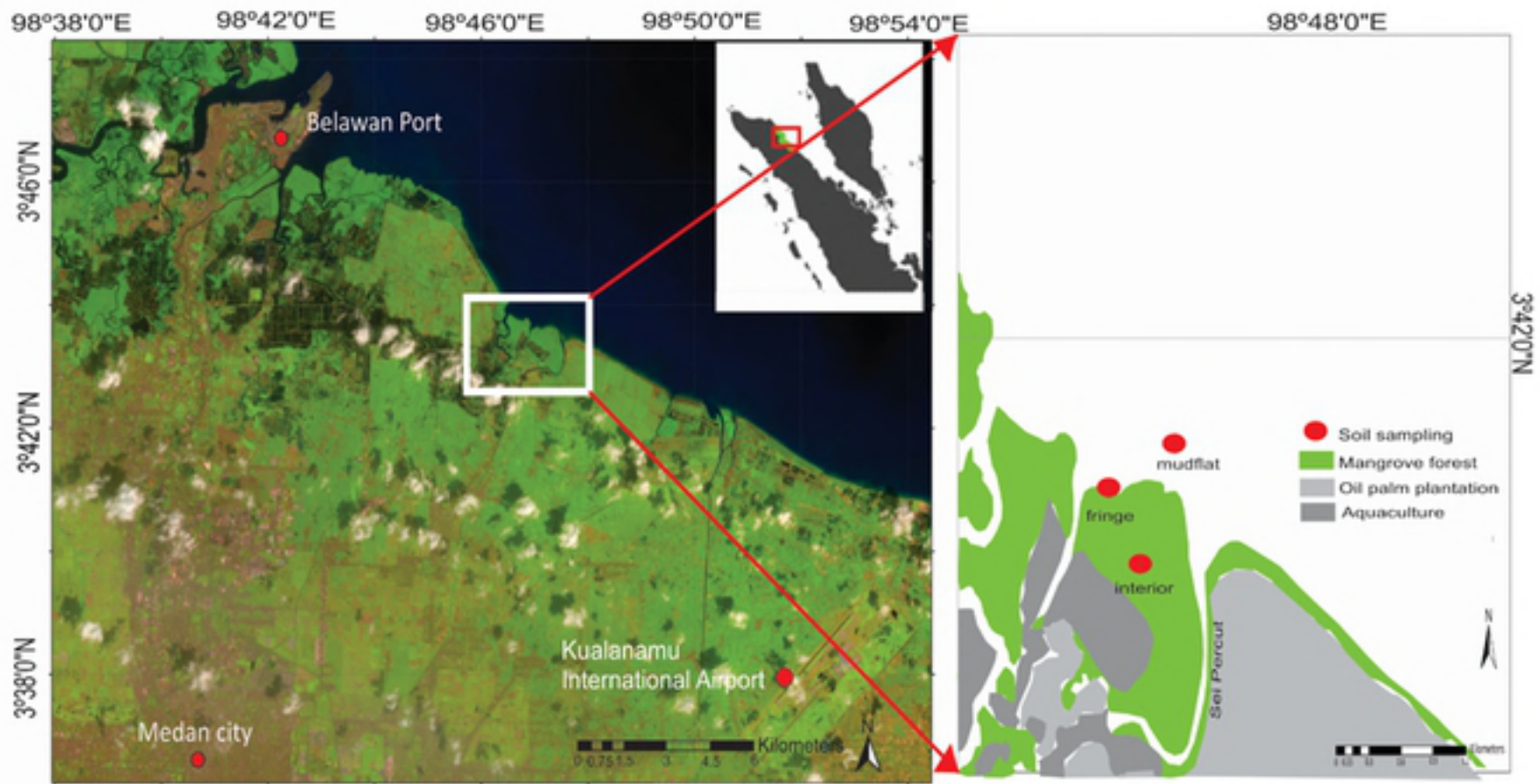
- 327 11. Adame MF, Neil D, Wright SF, and Lovelock CE. Sedimentation within and among mangrove forest  
328 along a gradient of geomorphological settings. *Estuarine, Coastal and Shelf Science*. 2010; 86:21 –  
329 30. doi:[10.1016/j.ecss.2009.10.013](https://doi.org/10.1016/j.ecss.2009.10.013)
- 330 12. Richards D and Friess DA. Rates and drivers of mangrove deforestation in Southeast Asia, 2000–  
331 2015. *PNAS*. 2015. doi:[10.1073/pnas.1510272113](https://doi.org/10.1073/pnas.1510272113).
- 332 13. Merrifield MA, Merrifield ST, and Mitchum GT. An anomalous recent acceleration of global sea level  
333 rise. *J Clim*. 2009; 22:5772-5781.
- 334 14. MacKenzie RA, Foulk PB, Klump JV, Weckerly K, Purbopuspito J, Murdiyarso D, Donato DC, and Nam  
335 VN. Sedimentation and belowground carbon accumulation rates in mangrove forest that differ in  
336 diversity and land use: a tale of two mangrove. *Wetlands Ecol Manage*. 2016. doi:[10.1007/s11273-](https://doi.org/10.1007/s11273-016-9481-3)  
337 [016-9481-3](https://doi.org/10.1007/s11273-016-9481-3)
- 338 15. Church JA, White NJ, Konikow LF, Domingues CM, Cogley JG, Rignot E, Gregory JM, van den Broeke  
339 MR, Monaghan AJ, and Velicogna I. Revisiting the earth's sea level and energy budgets from 1961 to  
340 2008. *Geophysical Research Letters*. 2011; 38. L18601. doi: [10.1029/2011GL048794](https://doi.org/10.1029/2011GL048794)
- 341 16. Ball MC, Cowan IR, and Farquhar GD. Maintenance of leaf temperature and the optimization of  
342 carbon gain in relation to water loss in a tropical mangrove forest. *Aus J Plant Physiol*. 1988; 15: 263-  
343 276.
- 344 17. Lovelock CE, Cahoon DR, Friess DA, Guntenspergen GR, Krauss KW, Reef R, Rogers K, Saunders ML,  
345 Sidik F, Swales A, Saintilan N, Thuyen LE Xuan, and Triet T. The vulnerability of Indo-Pacific mangrove  
346 forests to sea level rise. *Nature*. 2015. doi:[10.1038/nature15538](https://doi.org/10.1038/nature15538)
- 347 18. Sanders CJ, Santos IR, Silva-Filho EV, and Patchineelam SR. Mercury flux to estuarine sediments,  
348 derived from Pb-210 and Cs-137 geochronologies (Guaratube Bay, Brazil). *Marine Pollution Bulletin*.  
349 2006; 52: 1085-1089.



- 350 19. Sanders CJ, Smoak JM, Sanders LM, Waters MN, Patchineelam SR, and Ketterer ME. Intertidal  
351 mangrove mudflat <sup>240+239</sup>Pu signatures, confirming a <sup>210</sup>Pb geochronology on the southeastern coast  
352 of Brazil. *Journal Radioanal Nuclide and Chemical*. 2010; 283: 593-596.
- 353 20. Robbins JA and Edington DN. Determination of recent sedimentation rates in Lake Michigan using  
354 Pb-210 and Cs-137. *Geochimica et Cosmochimica Acta*. 1975; 39: 285-304.
- 355 21. Appleby PG. The calculation of lead-210 dates assuming a constant rate of supply of unsupported  
356 <sup>210</sup>Pb to the sediment. *CATENA*. 1978; (5): 1-8.
- 357 22. Marchio DA, Savarese Jr M, Bovard B, and Mistch WJ. Carbon sequestration and sedimentation in  
358 mangrove swamps influenced by hydrogeomorphic conditions and urbanization in Southwest  
359 Florida. *Forest*. 2016; 7: 116. doi:[10.3390/f7060116](https://doi.org/10.3390/f7060116)
- 360 23. Smoak JM, Breithaupt JL, Smith III TJ, and Sanders CJ. Sediment accretion and organic carbon burial  
361 relative to sea-level rise and storm events in two mangrove forests in Everglades National Park.  
362 *Catena*. 2012; 01876: 9
- 363 24. Ferland ME, Prairie YT, Teodoru CT, and del Giorgio PA. Linking organic carbon sedimentation, burial  
364 efficiency, and long-term accumulation in boreal lakes. *Journal of Geophysical Research:*  
365 *Biogeosciences*. 2014; 119: 836-847.
- 366 25. Drexler JZ and Ewel KC. Effect on the 1997-1998 ENSO-related drought on hydrology and salinity in a  
367 Micronesian wetland complex. *Estuaries*. 2001; 24(3): 347-356.
- 368 26. Ellison JC. Impact of sediment burial on mangroves. *Marine Pollution Bulletin*. 1998: 37; 420-426.
- 369 27. BPS SUMUT. *North Sumatra in Figs - 2015*. Badan Pusat Statistik Provinsi Sumatera Utara. Medan.  
370 2015. (In Indonesian).
- 371 28. Cossa D, Buscail R, Puig P, Chiffolean JF, Radakovitch O, Jeanty G, and Heussner S. Origin and  
372 accumulation of trace elements in sediments of the northwestern Mediterranean margin. *Chemical*  
373 *Geology*. 2014; 380: 61-73.

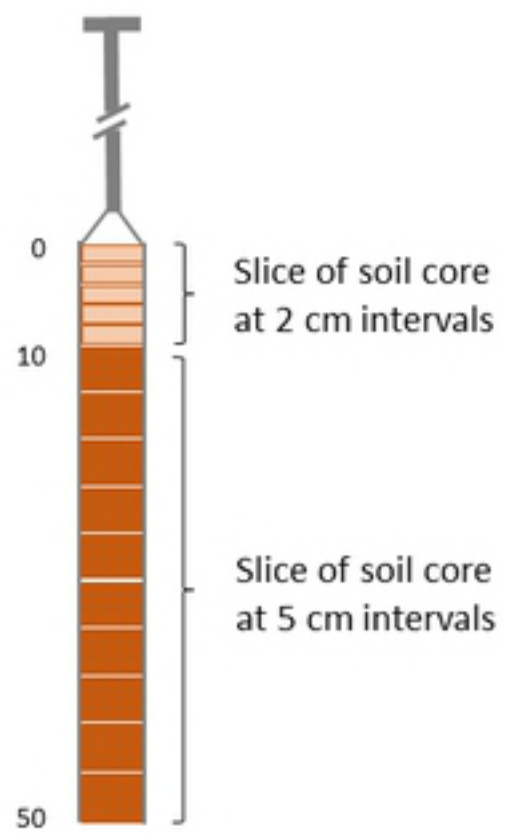
- 374 29. Alongi DM. Carbon cycling and storage in mangrove forests. *Annual Review of Marine Science*. 2014;  
375 6; 195-219.
- 376 30. Twilley RR, Chen RH, and Hargis T. Carbon sinks in mangroves and their implications to carbon  
377 budget of tropical coastal ecosystems. *Water, Air, and Soil Pollution*. 1992; 64: 265-288.
- 378 31. Alongi DM. Carbon sequestration in mangrove forest. *Carbon Management*. 2012; 3(3): 313-322.
- 379 32. Krauss KW, McKee KL, Lovelock CE, Cahoon DR, Saintilan N, Reef R, and Chen L. 2013. How  
380 mangrove forest adjust to rising sea level. Tansley review. *New Phycologist*. 2013.  
381 doi:[10.1111/nph.12605](https://doi.org/10.1111/nph.12605)
- 382 33. NOAA. Regional mean sea level rise (Andaman sea). 2014. [cited 2016 Oct 26]. Database : NOAA  
383 [internet]. Available from: [www.star.nesdis.noaa.gov/sod/lsa/SeaLevelRise/](http://www.star.nesdis.noaa.gov/sod/lsa/SeaLevelRise/)
- 384 34. McIvor AL, Spencer T, Möller I, and Spalding M. The response of mangrove soil surface elevation to  
385 sea level rise. Natural Coastal Protection Series: Report 3. Cambridge Coastal Research Unit Working  
386 Paper 42. 2013.
- 387 35. Cahoon DR, Hensel PF, Spencer T, Reed DJ, McKee KL, and Saintilan N. Coastal wetland vulnerability  
388 to relative sea level rise: wetland elevation trends and process control. *In: Wetlands and Natural  
389 Resource Management* (eds. Verhoeven JTA, Beltman B, Bobbink R, and Whigham DF): Ecological  
390 studies 190. Springer-Verlag, Berlin, Heidelberg. 2006. pp: 271-292.
- 391 36. Woodroffe CD, Rogers K, McKee KL, Lovelock CE, Mendelssohn IA, and Saintilan N. Mangrove  
392 sedimentation and response to relative sea level rise. *Annu. Rev. Mar. Sci.* 2016; (8): 243-266.
- 393 37. Cahoon DR and Lynch JC. Vertical accretion and shallow subsidence in a mangrove forest of  
394 southwestern Florida. *Mangroves and Salt Marshes*. 1997; 1: 173-186.
- 395 38. Furukawa K and Wolanski E. Sedimentation in mangrove forest. *Mangroves and Salt Marshes*. 1996;  
396 1(1): 3-10.

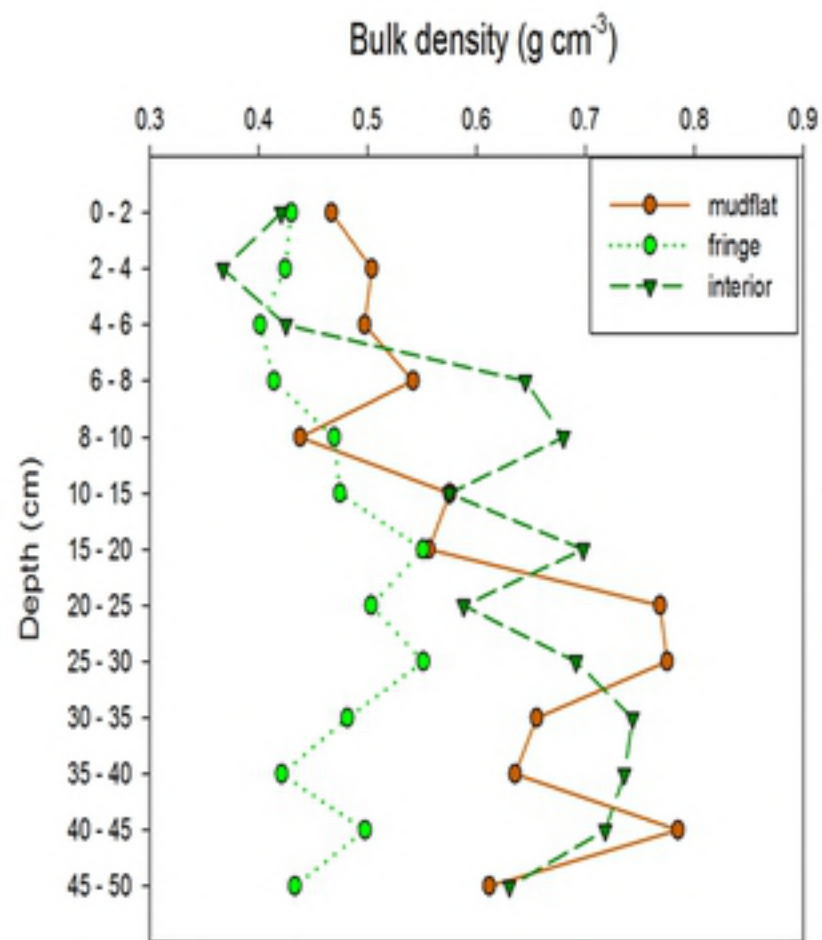
- 397 39. McLeod E, Chmura GL, Bouillon S, Salm R, Björk M, Duarte CM, Lovelock CE, Schlesinger WH, and  
398 Silliman BR. A blueprint for blue carbon: toward an improved understanding of the role of vegetated  
399 coastal habitats in sequestering CO<sub>2</sub>. *Front Ecol Environ*. 2011; 9(10): 552-560. doi:[10.1890/110004](https://doi.org/10.1890/110004)
- 400 40. Breithaupt JL, Smoak JM, Smith TJ, Sanders CJ, and Hoare A. Organic carbon burial rates in mangrove  
401 sediments: Strengthening the global budget. *Global Biogeochemical Cycles*. 2012; 26: GB3011.
- 402 41. Breithaupt JL, Smoak JM, Smith TJ, and Sanders CJ. Temporal variability of carbon and nutrient  
403 burial, sediment accretion, and mass accumulation over the past century in a carbonate platform  
404 mangrove forest of the Florida Everglades. *J. Geophys. Res. Biogeosci.* 2014; 119.  
405 doi:[10.1002/2014JG002751](https://doi.org/10.1002/2014JG002751)
- 406 42. Brunskill GJ, Zargorskis I, and Pfitzner J. Carbon burial rates in sediments and a carbon mass balance  
407 for the Herbert river region of the Great Barrier Reef continental shelf, North Queensland, Australia.  
408 *Estuarine, Coastal and Shelf Science*. 2002; 54: 677-700.
- 409 43. Callaway LC, DeLaune RD, and Patrick WH Jr. Sediment accretion rates from four coastal wetlands  
410 along the Gulf of Mexico. *Journal of Coastal Research*. 1997; 13(1): 181-191.
- 411 44. Sanders CJ, Smoak JM, Naidu A Sathy, Araripe DR, Sanders LM, and Patchineelam SR. Mangrove  
412 forest sedimentation and its reference to sea level rise, Cananea, Brazil. *Environ Earth Sci*. 2010;  
413 60:1291-1301.



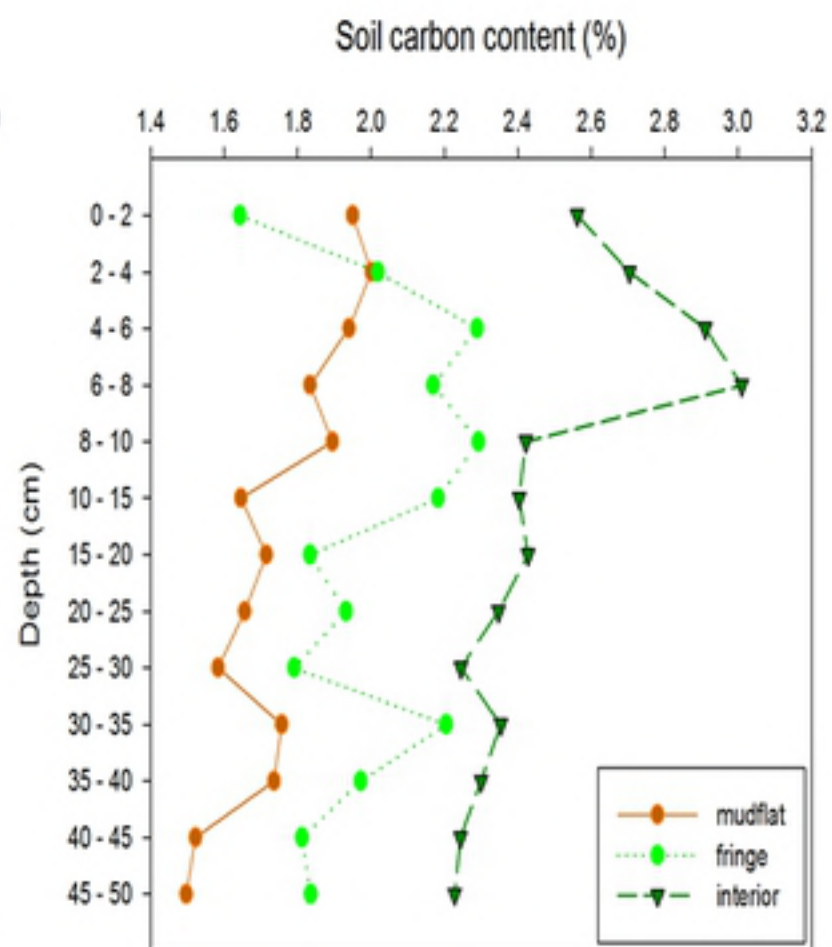
(a)

(b)

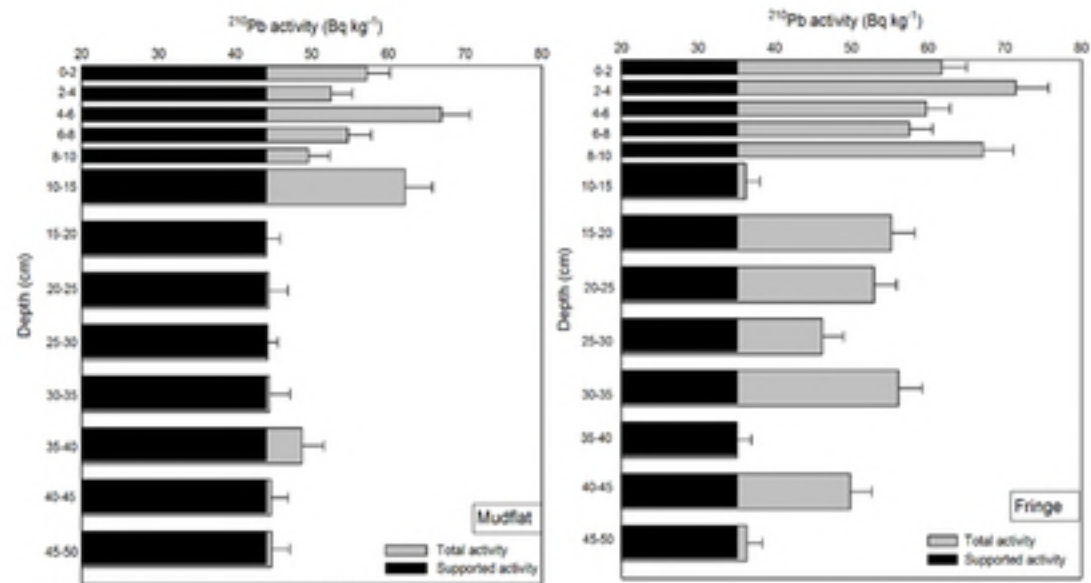




(a)

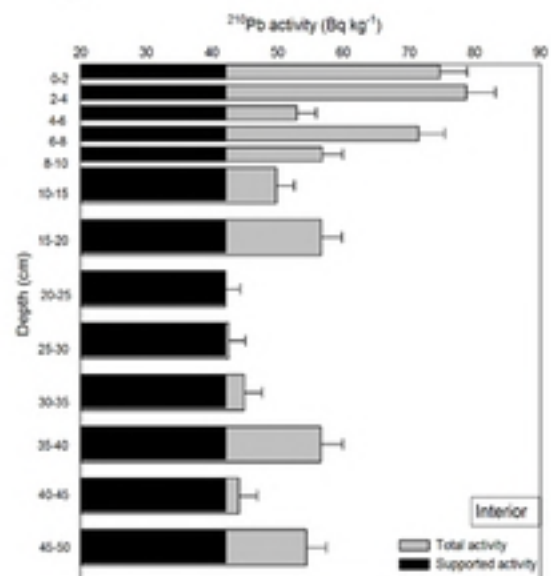


(b)



(a)

(b)



(c)

